

See discussions, stats, and author profiles for this publication at: <https://www.researchgate.net/publication/277941333>

Using radon as environmental tracer for the assessment of subsurface Non-Aqueous Phase Liquid (NAPL) contamination – A review

Article in *The European Physical Journal Special Topics* · May 2015

DOI: 10.1140/epjst/e2015-02402-3

CITATIONS

9

READS

165

1 author:



Michael Schubert

UFZ - Helmholtz Centre for Environmental Research

69 PUBLICATIONS 801 CITATIONS

SEE PROFILE

Some of the authors of this publication are also working on these related projects:



Isotope mass balance of lakes: regional perspectives [View project](#)

Using radon as environmental tracer for the assessment of subsurface Non-Aqueous Phase Liquid (NAPL) contamination – A review

M. Schubert^a

UFZ Helmholtz Centre for Environmental Research, Permoserstr. 15, 04318 Leipzig, Germany

Received 24 February 2015 / Received in final form 23 April 2015
Published online 10 June 2015

Abstract. The radioactive noble gas radon has an ambivalent nature: on the one hand is it of main concern with regard to radiation protection, on the other hand can it be applied as powerful tracer tool in various fields of applied geosciences. Due to its omnipresence in nature, its chemical and physical properties, and its uncomplicated detectability radon fulfils all requirements for being used as environmental tracer. This application is discussed in the paper with focus on the use of radon as tracer for subsurface contamination with Non-Aqueous Phase Liquids (NAPL). After a short introduction in the ambivalence and ubiquitous presence of radon in nature, the theoretical background of its suitability as NAPL tracer is summarized. Finally three potential applications are discussed. Background information and practical examples are given for (i) the investigation of residual NAPL contamination in soils, (ii) the investigation of residual NAPL contamination in aquifers and (iii) the monitoring of the remediation of dissolved NAPL contamination in groundwater. The presented information reveals that radon is an ideal tracer for the assessment of a wide range of subsurface NAPL contamination. Still, its application is not without restrictions. Problems may occur due to mineralogical heterogeneity of the soil or aquifer matrix. Furthermore, local changes in the permeability of the subsurface may be associated with preferential groundwater or soil gas flow paths bypassing isolated sub-domains of an investigated NAPL source zone. Moreover, NAPL aging may result in alterations in the composition of a complex NAPL mixture thus giving rise to significant changes of the radon partition coefficient between NAPL and water or soil gas. However, since radon shows a strong affinity to NAPLs in general, semi-quantitative results will always be possible.

1 Introduction

If the natural occurrence of radon is being discussed the element is rarely considered a useful component of soil gas or groundwater. The reason for that point of view is that

^a e-mail: michael.schubert@ufz.de

radon and its progeny are inhaled with every breath; while radon is exhaled again, part of the inhaled progeny gets trapped in the respiratory tract and the lungs. As the progeny undergoes further radioactive decay some of the short lived radionuclides (^{218}Po , ^{214}Po) emit alpha particles, which strike the sensitive lung tissue, potentially leading to the formation of cancerous cells. With the aim to quantify the related risk based on an extensive data pool Darby et al. [1] performed a collaborative analysis of data taken from 13 independent case studies. The results revealed that the risk of lung cancer increases steadily with increasing radon in air concentrations and that the famous quotation by Paracelsus “sola dosis facit venenum” (the dose makes the poison) does not seem to hold for radon. The determined linear dose/response relation between long-term radon exposure and cases of lung cancer did not suggest any lower threshold value.

However, in spite of the health related issues referred to above, radon can also be looked at from a completely different angle: not as a cause of problems but as a tool for tackling environmental challenges. During the last two decades a variety of novel applications based on the use of naturally occurring radon as aqueous or gaseous tracer appeared in the field of applied and environmental geosciences.

Motivation for the application of tracers in general is the difficulty to monitor certain subsurface processes directly. Another intention for using tracers is that most conventional subsurface survey approaches that are based on soil or groundwater sampling result in information that has to be considered point values only. Hence, their suitability for the characterization of large-scale and/or long-term processes is rather limited. As alternative, the application of tracers allows measurements at larger scales in both space and time [e.g. [2–5]]. In particular Environmental Tracers are suitable in the given context. They are defined as ubiquitously occurring natural or anthropogenic substances and/or physical indicators that are detectable in virtually all environments. In contrast to injected artificial tracers, environmental tracers have three key advantages: (i) they involve no risk of environmental contamination, (ii) they involve no perturbation to the system that is being studied, and (iii) they are suited to large-scale and/or long-term studies.

Radon is an element that is present in all soil gas and groundwater. Due to this omnipresence in nature, its chemical and physical properties, and its uncomplicated and precise detectability both on site and in the laboratory [6–10] radon fulfils practically all requirements for an application as environmental tracer. Prominent examples include approaches for (i) the investigation of groundwater migration processes [11, 12], (ii) surface water/groundwater interaction studies in marine [13–17] and freshwater systems [18–23], and (iii) the investigation of soil or groundwater contamination [24–30]. With the aim to call the attention onto this advantageous side of radon, the possibility of its application as environmental tracer for the evaluation of subsurface contamination with Non-Aqueous Phase Liquids (NAPL) is discussed in the paper.

2 The ubiquitous presence of radon in nature

The radioactive noble gas ^{222}Rn (hereafter referred to as radon) is produced via alpha-decay of its parent nuclide ^{226}Ra (hereafter referred to as radium). Since radium is present in virtually all mineral material, radon is produced constantly in every soil or aquifer matrix corresponding to the radium activity concentration of the mineral matrix (A_{Ra}). Alpha recoil is the most important driver for radon release from the mineral lattice into the open pore space, i.e. for its emanation from the mineral matrix. When a radium atom decays, an alpha particle is ejected and the newly formed radon atom recoils in the opposite direction [e.g. [31]]. The distance, which a newly formed radon atom is able to migrate do to its recoil is in a range between 0.02 and 0.07 μm

depending on the mineral structure [32]. Hence, the location of the decaying radium atom in the mineral grain (i.e. its distance to the grain surface) and the direction of recoil (toward the grain surface or the opposite way) determine whether the newly formed radon atom has a chance to enter the pore space or not. Emanation via diffusion is negligible since the diffusion coefficient of radon in mineral lattices (about $10\text{--}20\text{ cm}^2/\text{s}$; [32]) allows only diffusion lengths between 10^{-7} and $10^{-26}\text{ }\mu\text{m}$ [33]. The ratio between the number of radon atoms that emanate from a mineral matrix into the soil gas or groundwater filled pore space and the total number of radon atoms produced is expressed by the emanation coefficient (ε), a dimensionless and matrix-specific parameter that ranges between 0.1 and 0.7 and can normally be assumed to be around 0.25 [31].

Besides A_{Ra} and ε , the radon concentration in the pore space of an aquifer or soil (C_∞) depends on the porosity (n) and the bulk density (ρ_d) of the mineral matrix. The relationship, which describes the equilibrium radon concentration in the pore space as function of the four parameters is given with Eq. (1) [34].

$$C_\infty = \frac{\varepsilon A_{Ra} \rho_d}{n} \quad [\text{Bq}/\text{m}^3]. \quad (1)$$

Radon concentrations in soils or aquifers (i.e. in soil gas or groundwater, respectively) range generally between roughly 5 and $50\text{ kBq}/\text{m}^3$. That means that radon concentrations that are typically found in natural environments are in general considerably above the respective detection limits of modern (mobile) radon detectors.

Besides the omnipresence of radon in soil gas and groundwater, it is its generally inert behavior, which makes it a suitable tracer. Its affinity to fluorine or its bonding within some phenol clathrates, as it has been observed in laboratory experiments by Weigel [35], is generally of no relevance for on-site tracer applications. The same holds for radon adsorption onto activated coal, a characteristic that might become a problem if activated coal filters are used over a long time for soil gas remediation purposes without recycling [36]. Very dry soils tend to adsorb radon, an effect that becomes negligible if the water content exceeds only a few per cent and is hence in natural environments hardly ever of relevance [31]. Microbial metabolization of radon can be ruled out as radon sink term as well. Hence, the radon concentration in soil gas or groundwater is more or less constant in both space and time if a fairly homogeneous lithological composition of the soil or the aquifer is present. In an uncontaminated mineral matrix the radon concentration will only decrease due to the diffusive or advective escape of radon from the groundwater or the soil gas into the atmosphere (“exhalation”; [37–39]) (the radon partition coefficient between water and air at temperatures typically found in groundwater (at temperate latitudes) is about 0.35; [40, 41]). Hence, lateral or temporal radon anomalies in soil gas or groundwater that are not caused by changing lithological conditions can be used as indicators for processes or conditions that spatially or temporarily influence the subsurface radon distribution pattern. A prominent example of such influence is subsurface contamination with NAPL.

3 Radon as tracer for NAPL contamination assessment

3.1 Common challenges in NAPL contamination assessment

A major problem frequently encountered at (abandoned) industrial sites is soil or aquifer contamination with NAPL. Effective remediation planning and risk assessment necessitate the localization and quantification of both, the residual NAPL that

is present in the subsurface (“NAPL source zone”) and, in the case of aquifer contamination, the contaminants that occur dissolved in the groundwater (NAPL plume). While NAPL plumes can be investigated rather easily by straightforward groundwater sampling and (on-site) water analysis, NAPL source zones within an aquifer are harder to localize since they cannot easily be distinguished from the plume. That is due to their usually erratic and patchy shape, which complicates their investigation by conventional means, i.e. by groundwater or aquifer material sampling.

During the last two decades, several authors suggested the use of radon as environmental tracer for the localization and assessment of residual NAPL contamination in both soil [29,30,42] and aquifer [43–45,51]. It was shown that in soil and aquifer portions that are contaminated with residual NAPL (i.e. NAPL source zones) the preferential partitioning of radon into the residual organic phase results in a local radon deficit in soil gas or groundwater. The resulting radon deficit (with regard to the site specific radon background concentration) can be utilized as NAPL indicator. Hence, using radon as environmental tracer allows localizing a NAPL contaminated soil zone by carrying out a straightforward survey of the local radon distribution pattern in the soil gas. In the case of aquifer contamination radon allows on top of the localization a quantitative estimation of the NAPL contamination.

The magnitude of the radon deficit within a NAPL source zone in a soil or aquifer domain depends primarily (i) on the share of pore space that is occupied by residual NAPL and (ii) on the NAPL specific (temperature dependent) radon partition coefficient that is either applicable for soil gas ($K_{NAPL/SG}$) or groundwater ($K_{NAPL/W}$) as discussed in the following.

3.2 Radon partitioning behavior

3.2.1 The radon partition coefficient

The understanding of the radon partitioning between residual NAPL, soil gas and groundwater (or soil moisture) is of key importance if radon is to be used as quantitative NAPL tracer. On the one hand, the radon partitioning between soil gas (air) and water is well described and quantified [40]. The related partition coefficient ($K_{W/SG}$), which quantifies the ratio of the equilibrium radon concentrations in water (C_W) and soil gas (C_{SG}) depends on temperature and water salinity and can be determined as given in [41]. An equation that considers solely the temperature dependency and is hence applicable for most groundwaters and terrestrial surface waters was given by Weigel [35] (Eq. (2)).

$$K_{W/SG} = \frac{C_W}{C_{SG}} = f(T) = 0.105 + 0.405e^{-0.0502T[^\circ\text{C}]} \quad (2)$$

On the other hand, hardly any reliable radon solubility data is available for multi-component NAPL mixtures [26,40,45] even though a considerable quantity of radon data has been published for pure organic components [40,46]. However, knowledge of the related radon partition coefficients is mandatory if radon shall be used for quantitative NAPL contamination assessment of aquifers since complex NAPL mixtures such as gasoline, diesel fuel, and kerosene are the most frequently occurring contaminants in such cases.

For describing the radon solubility in NAPLs the Regular Solution Theory of Hildebrand and Scatchard can be applied, which uses Hildebrand's solubility parameter (δ) as molecular descriptor [47,48]. The general concept is based on the following observation [26] if NAPL specific radon solubilities (in terms of the partition coefficient $K_{NAPL/W}$) are plotted against the corresponding Hildebrand parameters of

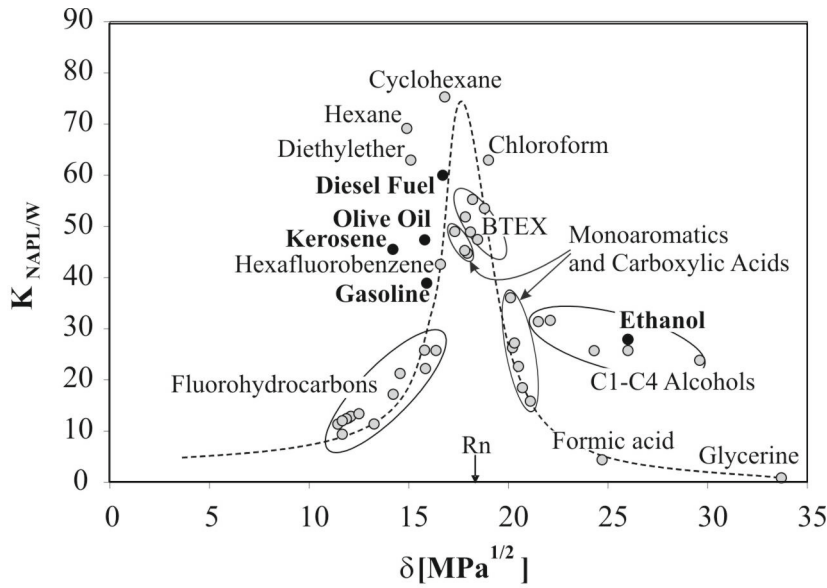


Fig. 1. Relationship $K_{NAPL/W}$ vs. δ for rough estimation of the radon solubility [26].

Table 1. $K_{NAPL/W}$ for olive oil and environmentally relevant complex NAPL mixtures.

	olive oil	diesel fuel	kerosene	gasoline
$K_{NAPL/W}$	45.5 ± 0.8	60.0 ± 1.3	47.4 ± 0.2	38.9 ± 0.9

the NAPLs, a sharp maximum is obtained at the Hildebrand parameter of radon ($18.1 \text{ MPa}^{1/2}$; valid for 298 K; [49]). Figure 1 illustrates the $K_{NAPL/W}$ vs. δ – relationship. The correlation allows a rough estimation of the radon solubility in a NAPL if the respective NAPL-specific Hildebrand parameter is known. Apart from that possibility of approximate theoretical prediction of the radon partition coefficient, experimental results revealed that at temperatures around 15°C radon partition coefficients between NAPL and water of about $K_{NAPL/W} = 40$ to 60 can be expected. Experimentally achieved values as given in [26] are summarized in Table 1.

3.2.2 Radon partitioning in the NAPL contaminated soil or aquifer matrix

Based on Eq. (1), Eq. (3) describes the equilibrium radon concentration of the soil gas (C_∞) within a NAPL contaminated soil volume. Defined shares (S) of the pore space are occupied by soil gas (S_{SG}), pore water (i.e. soil moisture; S_W) and NAPL (S_{NAPL}), respectively. The total fluid saturation of the pore space, i.e. $S_{NAPL} + S_W$, is given as S_F . Equation (3) considers the decrease of the air filled pore space (n) due to its occupation by the fluids and the partitioning of radon between the three phases. X_{NAPL} stands for the NAPL share of S_F (i.e. $S_{NAPL} + S_W = S_F = 1$).

$$C_\infty = \frac{\varepsilon A_{Ra} \rho_d}{n(1 - S_F + K_{W/SG} S_F (1 - X_{NAPL}) + K_{NAPL/SG} X_{NAPL} S_F)} \quad (3)$$

Figure 2 illustrates the theoretical dependence of C_∞ with increasing fluid saturation S_F of the pore space according to Eq. (3), the fluid being a mixture of water (soil moisture) and residual NAPL. The exemplary NAPL chosen for illustration

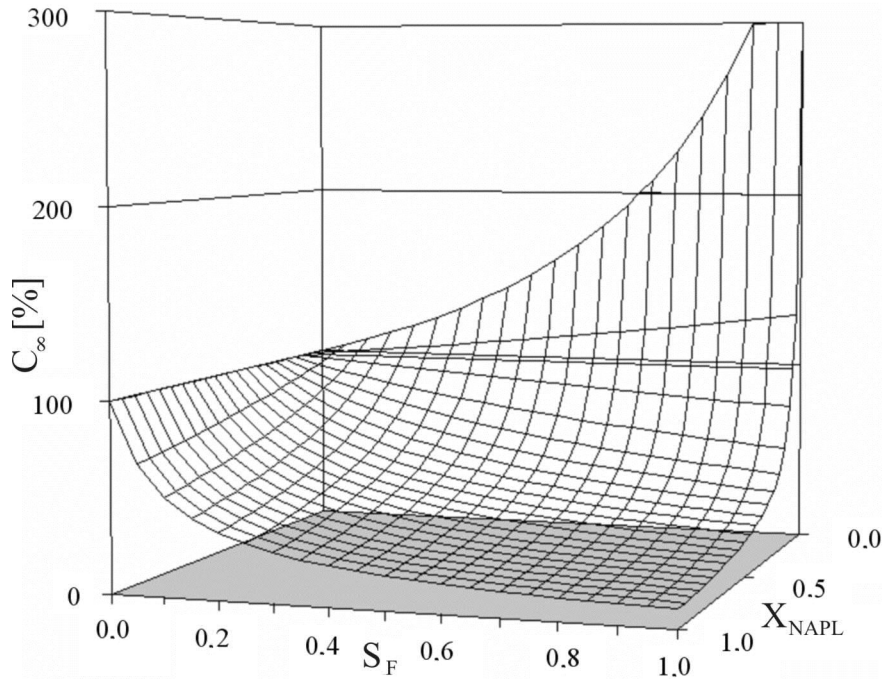


Fig. 2. Influence of residual NAPL contamination on the radon concentration of the soil gas.

is characterized by radon partition coefficient of $K_{NAPL/SG} = 10$. The plot illustrates that increasing NAPL saturation of the pore space (i.e. increasing S_F at high NAPL shares X_{NAPL}) leads to a significant reduction in the radon concentration in the soil gas, as expected. For instance at a 20% fluid saturation of the pore space with a 80% share of residual NAPL (i.e. $S_F = 0.2$, $X_{NAPL} = 0.8$) the equilibrium radon concentration in the soil gas is theoretically reduced to about 41% of the concentration that would have to be expected as background value for the uncontaminated soil (i.e. = 100%). At the same time it can be seen, that an increasing water saturation of the pore space without any noteworthy contamination leads to an increase of the equilibrium radon concentration in the soil gas, which is due to the reduction of the soil gas filled pore space (Eq. (1)). If only soil gas and NAPL are considered, i.e. if a soil with negligible soil moisture content is assumed ($X_{NAPL} = 1$), Eq. (3) reduces to Eq. (4). If no NAPL is present either ($S_{NAPL} = 0$) it reduces to Eq. (1).

$$C_{\infty} = \frac{\varepsilon A_{Ra} \rho_d}{n(1 - S_{NAPL} + K_{NAPL/SG} S_{NAPL})}. \quad (4)$$

In case of an aquifer contamination, i.e. in case of negligibly small volume of soil gas in the pore space, the radon concentration of the groundwater depends on the residual NAPL saturation of the pore space and on $K_{NAPL/W}$ of radon as given in Eq. (5). Again, if no NAPL is present ($S_{NAPL} = 0$) Eq. (5) reduces to Eq. (1).

$$C_{\infty} = \frac{\varepsilon A_{Ra} \rho_d}{n(1 - S_{NAPL} + K_{NAPL/W} S_{NAPL})}. \quad (5)$$

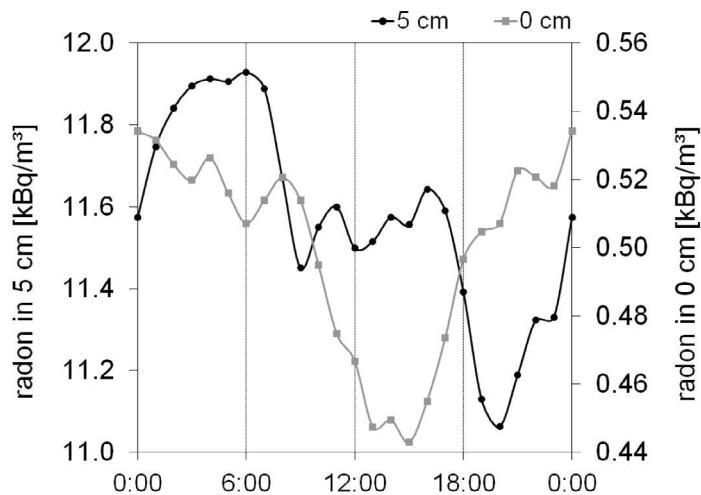


Fig. 3. Statistically recurring patterns of the radon concentrations at a depth of 5 cm and at the soil/air interface (0 cm) on basis of a 24 – hour period summarizing a 7 day time series [37].

4 Practical applications

4.1 Assessment of soil contamination with NAPL

Generally, if NAPL contamination of the soil zone is subject of investigation atmospheric influences on the radon distribution pattern in the subsurface have to be taken into account. The most influencing parameters are air pressure, wind speed and the temperature gradient at the soil/air interface [38,39,52]. In order to quantify the individual influences Schubert and Schulz [37] recorded the influential parameters simultaneously with radon concentration time-series in several depths of a defined soil column and at the soil/air interface over a seven day period. The results revealed distinct diurnal variations of the radon concentrations at the soil/air interface and in a depth of 5 cm (Fig. 3). In greater depths (down to 200 cm) no significant diurnal changes were detected (with a 7.5% stochastic error typical of the applied detection equipment). The diurnal radon pattern was found to correlate closely with the temperature gradient at the soil/air interface. It was concluded that mainly short-term temperature changes trigger the magnitude of the individual contributions of diffusive and convective radon migration to the overall radon transport. The diurnal pattern of the temperature gradient causes an increase in the radon concentration in the upper soil during the night and early morning hours and a decreased concentration in the evening. The radon concentration in the upper soil is also modulated by the diurnal variation of the wind speed, causing a concentration increase during the night (statistically characterized by lower wind speed) in particular at the soil/air interface.

In order to give a practical example for the assessment of soil contamination with NAPL a study carried out by Schubert et al. [29] shall be discussed briefly. An abandoned 120,000 m² airfield in northern Germany characterized by a homogeneous sandy soil was investigated. The contaminated zone had previously been investigated by means of soil coring revealing a heavy contamination with diesel fuel. The study aimed at confirming the results by means of a radon survey. For that purpose a total of 209 soil gas-samples were taken and analysed directly on site. All samples were taken from a depth of 70 cm to avoid meteorological influences on the soil gas composition. Figure 4 shows the resulting radon concentration pattern. The white dashed

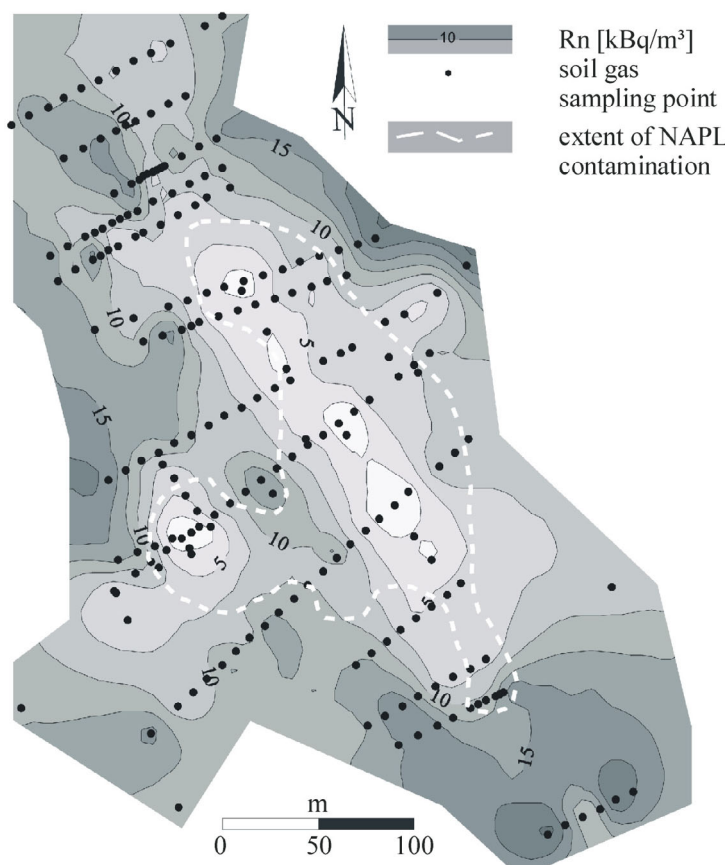


Fig. 4. Low radon concentrations of the soil gas indicate a kerosene contamination of the soil.

line encloses the contaminated area as it was localized previously by soil coring. As it can be seen, the radon distribution pattern reflects the NAPL contamination closely. Zones with low radon concentrations correspond to NAPL polluted areas. Background radon levels (around 15 kBq/m³) were found only outside the contaminated zone. Occasionally occurring higher radon concentrations are due to a tarmac covering of the ground and are, hence, not representative. The data allowed a more detailed localization of the contamination than the soil coring even though the radon survey was much less costly and time-consuming.

4.2 Assessment of aquifer contamination with NAPL

Besides soil contamination, NAPL contamination of aquifers is a common problem at any kind of industrial sites. While the actual contamination source is usually found close to the surface it is in particular dense NAPL (NAPL > 1 g/cm³) that is likely to migrate into the aquifer resulting in a NAPL source zone. Such NAPL source zones generally comprise small, disconnected residual blobs of organic liquid, typically between 1 and 10 pore throats in length, which are entrapped in the aquifer matrix by capillary forces and can typically occupy up to 20% of the pore space available [50]. Residual NAPL contamination of aquifers has to be considered as long term

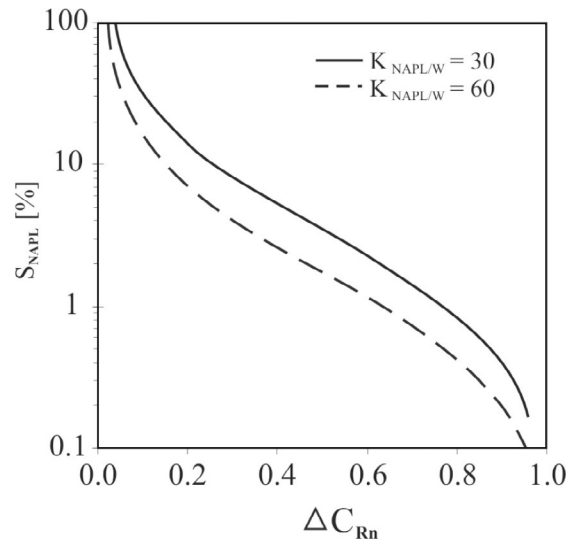


Fig. 5. NAPL saturation of the pore space (S_{NAPL} logarithmic scale!) vs. Radon Deficit Factor (ΔC_{Rn}) after Eq. (7).

sources of dissolved organic contaminants, which is mainly due to the in general low solubility of most DNAPLs.

Compared to soil contamination, the assessment of aquifer contamination with NAPL by using radon as a tracer has a general advantage: while the radon concentration in the gas filled pore space of an unsaturated soil can be subject to (temporal) variations as discussed above, no such influences are likely for the aquifer. That is due to the in general slow groundwater flow velocity (roughly 1–4 cm/d) and the very low radon diffusion coefficient in water of $1.16 \times 10^{-9} \text{ m}^2/\text{s}$ at 20°C (compared to air: $1.20 \times 10^{-5} \text{ m}^2/\text{s}$ at 20°C). Hence neither advection nor diffusion/dispersion plays a significant role for radon distribution patterns in saturated aquifers. At steady-state conditions, i.e. at complete radon partitioning between water and NAPL, a constancy of C_∞ as function of time can be assumed. Based on Eq. (5) a dimensionless Radon Deficit Factor ΔC_{Rn} can be derived ($0 < \Delta C_{Rn} < 1$), which allows direct comparison of the radon background concentration (i.e. $S_W = 1$) to the radon concentration in the contaminated but otherwise identical aquifer.

$$\Delta C_\infty = \frac{C_\infty(S_W < 1)}{C_\infty(S_W = 1)} = \frac{1}{K_{NAPL/W} - K_{NAPL/W}S_W + S_W}. \quad (6)$$

After rearrangement $(S_{NAPL} + S_W = 1)S_{NAPL}$ can be quantified as function of the determined Radon Deficit Factor as given in Eq. (7).

$$S_{NAPL} = \frac{1 - \Delta S_\infty}{\Delta C_\infty K_{NAPL/W} - \Delta C_\infty}. \quad (7)$$

Figure 5 illustrates the decrease of the Radon Deficit Factor with increasing NAPL saturation of the pore space (logarithmic scale). Plots are given for two partition coefficients $K_{NAPL/W}$. It becomes obvious that the radon concentration is most sensitive to changes in S_{NAPL} at low NAPL saturations ($S_{NAPL} < 5\%$) and not very sensitive above NAPL saturations of about $S_{NAPL} > 10\%$ [27].

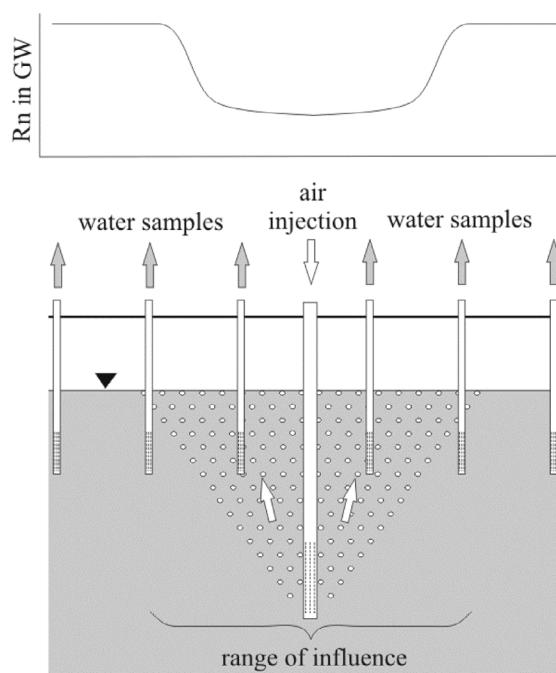


Fig. 6. Schematic sketch of the principle of using radon as IAS efficiency indicator; not to scale [24].

4.3 Evaluation of the efficiency of groundwater remediation by in situ air sparging

Radon cannot only be applied as tracer for residual NAPL contamination but also in the case of groundwater contamination with dissolved NAPLs. A common approach for remediation of groundwater contamination with volatile organic compounds (VOCs) is contaminant stripping by means of in situ air sparging (IAS). Within the physical range of the air sparging, i.e. within the range in which the air bubbles rise through the contamination plume, the VOCs partition from the water into the injected air and are thereby stripped from the groundwater. The stripped VOCs are carried into the overlying vadose soil zone, where they are collected by means of air pumps (Fig. 6).

Progress assessment of such remediation measure necessitates information (i) on the spatial range of the IAS influence and (ii) on temporal variations of the IAS efficiency. In a study published by Schubert et al. [24] it was shown that radon can be used as suitable environmental tracer for achieving the related information. Due to the distinct water/air partitioning of radon and due to its straightforward on-site detectability, the radon distribution pattern in the groundwater can be used for assessing the progression of an IAS measure as a function of space and time.

The study was carried out at a former industrial site in Central Germany. During decades of production storage tanks and pipelines had led to a considerable large-scale NAPL groundwater contamination. For the pilot study an air injection well (AS) was chosen, which was surrounded by seven groundwater sampling wells (SW). The IAS measure was carried out continuously for six months. During the procedure five sampling campaigns were carried out. Four weeks were allowed between each two

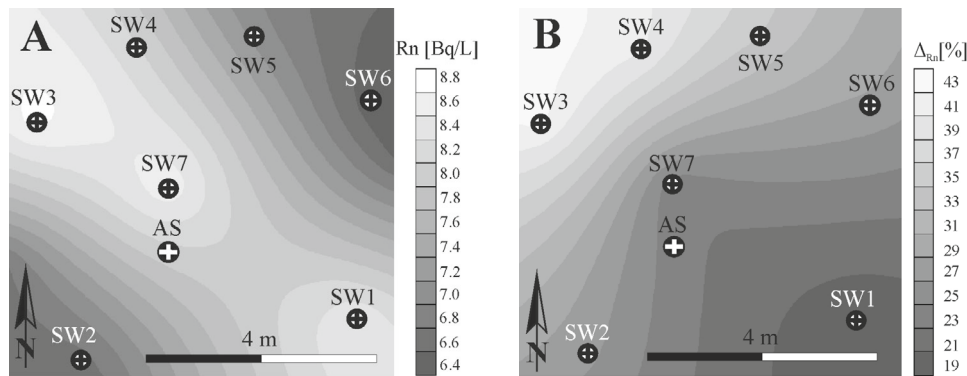


Fig. 7. Spatial radon distribution patterns around the air injection well (AS) without IAS influence (radon background, 7A) and during the IAS procedure (7B).

consecutive sampling campaigns. The radon concentration of the groundwater was measured immediately on site.

The achieved data allowed a twofold evaluation of the IAS efficiency: (i) an assessment of its range of influence and (ii) an evaluation of temporal variations. Figure 7 illustrates the radon distribution pattern at the site without any sparging influence (A) and during the remediation measure (B). Figure 7A indicates a linear geologic structure running NW-SE with inhomogeneities in the mineralogical aquifer composition that result in a distinct pattern of the radon background concentration in the groundwater. That was taken into consideration by using well-specific background-normalized radon concentration rather than absolute radon values for data evaluation. Figure 7B illustrates the Rn distribution pattern averaged over the entire period of air sparging, i.e. averaged over all five sampling campaigns. The plot shows a heterogeneous distribution of the IAS influence around the injection well. That spatial variability of the stripping efficiency is most likely due to an inhomogeneous permeability distribution within the aquifer. For instance, the data recorded at well SW7 indicate a comparably poor IAS efficiency despite the fact that SW7 is the sampling well closest to the injection well. A general conclusion that can be drawn from the results is that the efficiency of the air sparging measure is limited, i.e. that the accessibility of the saturated zone for the injected air varies spatially significantly. The data reveals that a circularly distributed sparging cone around the injection well, as it could be expected theoretically (cf. Fig. 6), has not developed. In Fig. 8 the temporal variability of the IAS efficiency is illustrated for all seven wells. The data shows that the IAS efficiency was most constant well SW4. In the neighboring wells SW3 and SW5 the average radon concentrations decreased to approximately the same level but the observed IAS efficiency is not as consistent with time. A reason for a varying efficiency can be a sparging induced change of porosity within the aquifer. Pathways can be clogged by air bubbles, thus altering air accessibility and flow paths through the aquifer (air clogging). Sampling wells SW1 and SW2 were located south of the air injection well, i.e. opposite to the wells discussed above. The radon concentrations detected here showed temporal patterns, with the lowest concentrations in the middle of the remediation measure. That indicates that the stripping of radon (and hence of VOCs) was somewhat delayed and did not reach the intensity observed in northern wells, which was attributed to the lower permeability and to the resulting reduced accessibility of that part of the aquifer to the injected air (cf. Fig. 7B).

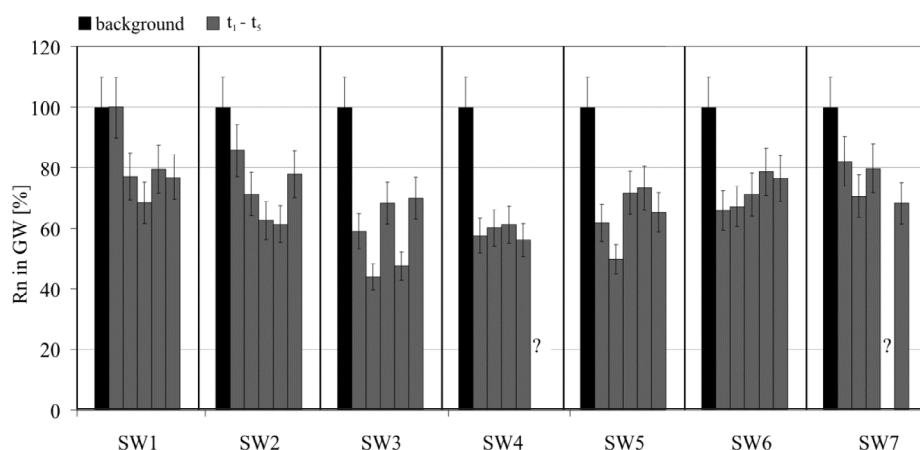


Fig. 8. Temporal variability of the air sparging efficiency illustrated for seven wells for the five sampling campaigns t_1 – t_5 .

5 Conclusion

The presented background information and data sets show that radon can ideally be applied as environmental tracer for the assessment of subsurface NAPL contamination both in soils and aquifers. The key property of the noble gas is its very strong affinity to a wide range of pure NAPLs and NAPL mixtures. A key advantage of its use is its uncomplicated and quick detectability by means of mobile detection equipment. However, in spite of this the presented approaches are not applicable without restrictions. Problems may occur due to mineralogical heterogeneity of the soil or aquifer matrix, which complicates final data assessment. The possibility of a non-homogeneous radium concentration of the mineral matrix has always to be taken into account since radon might therefore not be produced uniformly throughout the investigated portion of the subsurface. Furthermore, local changes in the subsurface permeability may be associated with preferential flow paths of soil gas or groundwater bypassing isolated sub-domains of the investigated NAPL contamination. Note also that NAPL aging may lead to considerable alterations in the composition of a complex NAPL mixture thus giving rise to a significant change of the radon partition coefficient of the remaining residual NAPL. The experimentally achieved partition coefficients summarized in the paper can only be considered as approximate values. However, since radon shows a strong affinity to NAPLs in general, semi-quantitative results will be possible.

References

1. S. Darby, D. Hill, A. Auvinen, J.M. Barros-Dios, H. Baysson, et al., *Brit. Med. J.* **330**, 223 (2005)
2. W. Käss, *Tracing Technique in Geohydrology* (Balkema, Rotterdam, Netherlands, 1998)
3. G.A. Whitley, D.C. McKinney, G.A. Pope, B.A. Rouse, N.E. Deeds, *J. Environ. Eng.* **125**, 574 (1999)
4. W.S. Moore, J.L. Sarmiento, R.M. Key, *Nature Geosci.* **1**, 309 (2008)
5. M.L. Brusseau, N.T. Nelson, M.S. Costanza-Robinson, *Vadose Zone Journal* **2**, 138 (2003)
6. M. Schubert, A. Paschke, D. Bednorz, W. Bürkin, T. Stieglitz, *Environ. Sci. Technol.* **46**, 8945 (2012a)

7. A. Schmidt, M. Schlüter, M. Melles, M. Schubert, *Appl. Radiat. Isotopes*, **66**, 1939 (2008)
8. M. Schubert, A. Schmidt, A. Paschke, A. Lopez, M. Balcázar, *Radiat. Meas.* **43**, 111 (2008b)
9. M. Schubert, W. Bürkin, P. Peña, A. Lopez, M. Balcázar, *Radiat. Meas.* **41**, 492 (2006)
10. M. Schubert, J. Kopitz, S. Chalupnik, *J. Environ. Radioactiv.* **134**, 109 (2014b)
11. M. Schubert, L. Brüggemann, M. Schirmer, K. Knöller, *Water Resour. Res.* **47**, W03512 (2011a)
12. H. Hamada, *J. Environ. Radioactiv.* **47**, 1 (2000)
13. M. Schubert, J. Scholten, A. Schmidt, J.F. Comanducci, M.K. Pham, U. Mallast, K. Knöller, *Water* **6**, 584 (2014a)
14. W.C. Burnett, H. Dulaiova, *J. Environ. Radioactiv.* **69**, 21 (2003)
15. J.E. Cable, W.C. Burnett, J.P. Chanton, G. Weatherly, *Earth Planet. Sci. Lett.* **144**, 591 (1996)
16. J.E. Cable, W.C. Burnett, J.P. Chanton, G.L. Weatherly, *Earth Planet. Sci. Lett.* **144**, 591 (1996)
17. D.R. Corbett, K. Dillon, W.C. Burnett, J. Chanton, *Limnol. Oceanogr.* **45**, 1546 (2000)
18. A. Schmidt, J.J. Gibson, I.R. Santos, M. Schubert, K. Tattrie, H. Weiss, *Hydrol. Earth Syst. Sci.* **14**, 79 (2010)
19. A. Schmidt, C.E. Stringer, U. Haferkorn, M. Schubert, *Environ. Geol.* **56**, 855 (2009)
20. A. Schmidt, M. Schubert, *Isot. Environ. Healt. S.* **43**, 387 (2007)
21. D.R. Corbett, W.C. Burnett, P.H. Cable, *J. Hydrol.* **203**, 209 (1997)
22. E. Hoehn, H.R. von Gunten, *Water Resour. Res.* **25**, 1795 (1989)
23. M. Schubert, H.C. Treutler, H. Weiss, J. Dehnert, in *Proceedings of the International Conference on Isotopes in Environmental Studies – Aquatic Forum 2004* (Monte-Carlo, Monaco, 2004)
24. M. Schubert, A. Schmidt, K. Müller, H. Weiß, *J. Environ. Radioactiv.* **102**, 193 (2011b)
25. M. Schubert, M. Balczar, A. Lopez, P. Peña, J.H. Flores, K. Knöller, *Isot. Environ. Healt. S.* **43**, 215 (2007)
26. M. Schubert, K. Lehmann, A. Paschke, *Sci. Total Environ.* **376**, 306 (2007b)
27. M. Schubert, A. Paschke, S. Lau, W. Geyer, K. Knöller, *Environ. Pollut.* **145**, 920 (2007c)
28. H.C. Treutler, G. Just, M. Schubert, H. Weiß, *J. Radioanal. Nucl. Ch.* **272**, 583 (2007)
29. M. Schubert, P. Peña, M. Balcázar, R. Meissner, A. Lopez, J.H. Flores, *Radiat. Meas.* **40**, 633 (2005)
30. M. Schubert, K. Freyer, H.C. Treutler, H. Weiß, *J. Soils Sediments* **1**, 217 (2001)
31. W.W. Nazaroff, A.V. Nero, *Radon and its Decay Products in Indoor Air* (John Wiley & Sons, New York/NY/USA, 1988)
32. A.B. Tanner, in *Proceedings of the International Symposium on the Natural Radiation Environment*, edited by T.F. Gesell, W.M. Lowder (US Department of Commerce, National Technical Information Service, Springfield/VA/USA, 1980)
33. W.W. Nazaroff, *Rev. Geophys.* **30**, 137 (1992)
34. J.N. Andrews, D.F. Wood, *Transactions of the Institution of Mining and Metallurgy* **B81**, 198 (1972)
35. F. Weigel, *Chemiker-Zeitung* **102**, 287 (1978)
36. B. Richter, W. Roßbander, in *Tagungsband des 9. Conulaqua Workshop zu innovativen Verfahren in der Erkundung, Bewertung* (Gefahrenabwehr bei Altlasten, Dresden/Deutschland, 1997)
37. M. Schubert, H. Schulz, *Health Phys.* **83**, 91 (2002)
38. H. Zafrir, S.M. Barbosa, U. Malik, *Radiat. Meas.* **49**, 39 (2013)
39. S.M. Barbosa, H. Zafrir, U. Malik, O. Piatibratova, *Geophys. J. Int.* **182**, 829 (2010)
40. H.L. Clever, *Solubility data series, Vol. 2: Krypton, Xenon and Radon gas solubilities*. International Union of Pure and Applied Chemistry (Pergamon Press, Oxford/UK, 1979)
41. M. Schubert, A. Paschke, E. Lieberman, W.C. Burnett, *Environ. Sci. Technol.* **46**, 39053911 (2012b)

42. P. Höhener, H. Surbeck, *Vadose Zone Journal* **3**, 1276 (2004)
43. B.M. Davis, J.D. Istok, L. Semprini, *J. Contam. Hydrol.* **78**, 87103 (2005)
44. L. Semprini, O.S. Hopkins, B.R. Tasker, *Transport Porous Med.* **38**, 223 (2000)
45. D. Hunkeler, E. Hoehn, P. Höhener, J. Zeyer, *Environ. Sci. Technol.* **31**, 3180 (1997)
46. C. Lewis, P.K. Hopke, J. Stukel, *Ind. Eng. Chem. Res.* **26**, 356 (1987)
47. A.F.M. Barton, *Handbook of solubility parameters and other cohesion parameters*, 2nd edition (CRC Press, Boca Raton/FL/USA, 1991)
48. J.M. Prausnitz, R.E. Lichtenthaler, E.G. de Azevedo, *Molecular thermodynamics of fluid phase equilibria*, 2nd Ed. (Prentice Hall, Englewood Cliffs/NJ/USA, 1986)
49. J.M. Prausnitz, F.H. Shair, *AIChE J.* **7**, 682 (1961)
50. J.W. Mercer, R.M. Cohen, *J. Contam. Hydrol.* **6**, 107 (1990)
51. B.M. Davis, J.D. Istok, L. Semprini, *J. Contam. Hydrol.* **58**, 129 (2002)
52. E. Strandén, A.K. Kolstad, B. Lind, *Health Phys.* **47**, 480 (1984)